BMP-9-induced osteogenic differentiation of mesenchymal progenitors requires functional canonical Wnt/β-catenin signalling

Ni Tang [a, b], Wen-Xin Song [b], Jinyong Luo [a, b], Xiaoji Luo [a, b], Jin Chen [a, b], Katie A. Sharff [b], Yang Bi [a, b], Bai-Cheng He [a, b], Jia-Yi Huang [a, b], Gao-Hui Zhu [a, b], Yu-Xi Su [a, b], Wei Jiang [b], Min Tang [a], Yun He [a, b], Yi Wang [a, b], Liang Chen [a, b], Guo-Wei Zuo [a, b], Jikun Shen [b], Xiaochuan Pan [c], Russell R. Reid [b], Hue H. Luu [b], Rex C. Haydon [b], Tong-Chuan He [a, b, *]

[a] *The Second Affiliated Hospital and the Key Laboratory of Diagnostic Medicine designated by the Chinese Ministry of Education, Chongqing Medical University, Chongqing, China*
[b] *Molecular Oncology Laboratory, Department of Surgery, The University of Chicago Medical Center, Chicago, IL, USA*
[c] *Department of Radiology, The University of Chicago Medical Center, Chicago, IL, USA*

Received: July 15, 2008; Accepted: October 21, 2008

Abstract

Bone morphogenetic protein 9 (BMP-9) is a member of the transforming growth factor (TGF)-β/BMP superfamily, and we have demonstrated that it is one of the most potent BMPs to induce osteoblast differentiation of mesenchymal stem cells (MSCs). Here, we sought to investigate if canonical Wnt/β-catenin signalling plays an important role in BMP-9-induced osteogenic differentiation of MSCs. Wnt3A and BMP-9 enhanced each other's ability to induce alkaline phosphatase (ALP) in MSCs and mouse embryonic fibroblasts (MEFs). Wnt antagonist FrzB was shown to inhibit BMP-9-induced ALP activity more effectively than Dkk1, whereas a secreted form of LPR-5 or low-density lipoprotein receptor-related protein (LRP)-6 exerted no inhibitory effect on BMP-9-induced ALP activity. β-Catenin knockdown in MSCs and MEFs diminished BMP-9-induced ALP activity, and led to a decrease in BMP-9-induced osteocalcin reporter activity and BMP-9-induced expression of late osteogenic markers. Furthermore, β-catenin knockdown or FrzB overexpression inhibited BMP-9-induced mineralization *in vitro* and ectopic bone formation *in vivo*, resulting in immature osteogenesis and the formation of chondrogenic matrix. Chromatin immunoprecipitation (ChIP) analysis indicated that BMP-9 induced recruitment of both Runx2 and β-catenin to the osteocalcin promoter. Thus, we have demonstrated that canonical Wnt signalling, possibly through interactions between β-catenin and Runx2, plays an important role in BMP-9-induced osteogenic differentiation of MSCs.

Keywords: BMPs • BMP-9 • canonical Wnt signalling • β-catenin • mesenchymal stem cells • osteogenic differentiation

Introduction

Bone morphogenetic protein 9 (BMP-9) (also known as growth differentiation factor 2, or GDF-2) is a member of the transforming growth factor (TGF)-β/BMP superfamily [1–7]. BMP-9 was first identified in the developing mouse liver [8], and its roles include inducing and maintaining the cholinergic phenotype of embryonic basal forebrain cholinergic neurons [9], inhibiting hepatic glucose production and inducing the expression of key enzymes of lipid metabolism [10], and stimulating murine hepcidin 1 expression [11]. However, the functional role of BMP-9 in the skeletal system is largely unknown. Upon analysing the 14 types of BMPs, we found that BMP-9 is one of the most potent BMPs in inducing osteogenic differentiation of mesenchymal stem cells (MSCs) both *in vitro* and *in vivo* [6, 12–16]. We further demonstrated that BMP-9 regulates a distinct set of downstream targets that may play a role in regulating BMP-induced osteoblast differentiation of MSCs [6, 14–17]. However, the molecular mechanism underlying the BMP-9-induced osteogenic differentiation of MSCs remains to be elucidated.

*Correspondence to: T.-C. HE, M.D., Ph.D.,
Molecular Oncology Laboratory,
The University of Chicago Medical Center, 5841 South Maryland Avenue,
MC 3079, Chicago, IL 60637, USA
Tel.: (773) 702-7169
Fax: (773) 834-4598
E-mail: tche@surgery.bsd.uchicago.edu

doi:10.1111/j.1582-4934.2008.00569.x

MSCs are adherent bone marrow stromal cells that can self-renew and differentiate into osteogenic, chondrogenic, adipogenic and myogenic lineages [7, 18–22]. Several signalling pathways have been implicated in regulating stem cell self-renewal and lineage commitment [23–27]. Osteogenic differentiation is under the control of hormonal and local factors converging onto a finite number of transcriptional regulators that ultimately determine the fate of cells committing to the osteogenic lineage [7, 28]. BMPs play an important role in stem cell biology [29, 30], as well as in regulating cell proliferation and differentiation during development [1, 3, 4]. Genetic disruptions of BMPs have resulted in skeletal and extraskeletal abnormalities [1, 31]. Although not well understood, BMPs are involved in regulating osteoblast differentiation and bone formation [5, 7, 32, 33].

Wnt/β-catenin signalling also plays an important role in skeletal development and osteoblast differentiation [7, 24, 28, 34–38]. Wnts are a family of secreted proteins that regulate many embryonic processes [7, 35, 39]. They bind to their cognate receptor frizzled (Fz) and LRP-5/6 co-receptors, and activate distinct signalling pathways, including the canonical β-catenin pathway. Wnt antagonists FrzB and Dkk1 inhibit the binding of Wnt ligands to their receptors. In the absence of Wnt signalling, β-catenin is degraded by the proteasome system after GSK-3β dependent phosphorylation. In the presence of Wnt signalling, unphosphorylated β-catenin accumulates in the cytoplasm and translocates into the nucleus where it associates with Tcf/LEF transcription factors to regulate the expression of target genes [27, 40–43]. Mutations in LRP-5 affect skeletal development and bone mass acquisition [44–46]. Studies from genetically manipulated animal models suggest that high levels of canonical Wnt/β-catenin with the presence of Runx2 may promote osteoblastogenesis at the expense of chondrocyte differentiation [35, 38]. A recent report has demonstrated that β-catenin signalling plays a disparate role in different phases of fracture repair [47], suggesting that Wnt/β-catenin may play a similar but distinct role in skeletogenesis *versus* bone regeneration. Conflicting results have indicated that canonical Wnt/β-catenin may inhibit osteogenic differentiation [48–52], and non-canonical Wnts were also shown to promote osteogenic differentiation [53, 54]. Thus, the downstream events following the activation of Fz/LRP-5/6 receptors and the precise function of β-catenin in osteoblasts remain to be fully elucidated.

In this report, we sought to determine whether canonical Wnt/β-catenin signalling plays an important role in mediating BMP-9-induced osteogenic differentiation of MSCs. We found that both Wnt3A and BMP-9 effectively induced alkaline phosphatase (ALP) activity and enhanced each other's ability to induce ALP activity in MSCs. Among the Wnt signalling inhibitors tested, FrzB was shown to inhibit BMP-9-induced ALP activity most effectively. While stabilized β-catenin enhanced BMP-9-induced ALP activity, RNAi-mediated silencing of β-catenin diminished the BMP-9-induced early stage of osteogenic differentiation. We further demonstrated that β-catenin enhanced BMP-9 or Runx2-induced osteocalcin promoter-based reporter activity, yet silencing β-catenin led to a decrease in BMP-9-induced osteocalcin reporter activity, and a decrease in BMP-9-induced expression of osteocalcin and osteopontin. Knockdown of β-catenin or overexpression of FrzB inhibited BMP-9-induced ectopic bone formation *in vivo*, resulting in a chondrogenic phenotype. Chromatin immunoprecipitation (ChIP) analysis indicated that BMP-9 induced the recruitment of both Runx2 and β-catenin to the osteocalcin promoter. Thus, these results indicate that canonical Wnt signalling, possibly through β-catenin interaction with Runx2, is critical in BMP-9-induced osteogenic differentiation of MSCs.

Materials and methods

Cell culture and chemicals

HEK293, HCT116 and C3H10T1/2 cell lines were obtained from ATCC (Manassas, VA, USA). HEK293 cells were maintained in complete Dulbecco's Modified Eagle's Medium (DMEM) supplemented with 10% foetal calf serum (FCS, Hyclone, Logan, UT, USA), 100 units/ml penicillin, and 100 μg/ml streptomycin at 37°C in 5% CO_2. C3H10T1/2 cells were maintained in Basal Medium Eagle in Earle's BSS, supplemented with 10% FCS, 100 units/ml penicillin and 100 μg/ml streptomycin at 37°C in 5% CO_2. HCT116 cells were maintained in McCoy's 5A medium, supplemented with 10% FCS, 100 units/ml penicillin and 100 μg/ml streptomycin at 37°C in 5% CO_2. Unless indicated otherwise, all chemicals were purchased from Sigma-Aldrich or Fisher Scientific.

Preparation of mouse embryonic fibroblasts (MEFs)

MEFs were isolated from post-coitus day 13.5 mice, as previously described [55]. Each embryo was dissected into 10 ml sterile phosphate buffered saline (PBS), voided of its internal organs, and sheared through an 18-gauge syringe in the presence of 1 ml 0.25% trypsin and 1 mM EDTA. After 15 min. incubation with gentle shaking at 37°C, DMEM with 10% FCS was added to inactivate trypsin. The cells were plated on 100-mm dishes and incubated for 24 hrs at 37°C. The adherent cells were used as MEF cells; aliquots were kept in a liquid nitrogen tank. All MEFs used in this study were within five passages.

Selection and construction of RNAi silencing vectors

We used our recently developed pSOS system to select and validate efficacious short interfering double-stranded RNA (siRNA) target sites of mouse β-catenin [56], and designed three pairs of oligonucleotides containing siRNA target sites for the coding region of mouse β-catenin using Dharmacon's *siDESIGN* program (Supporting Table S1). The oligo pairs were annealed and subcloned into the *Sfi* I site of pSES, resulting in adenoviral shuttle vectors pSES-simBCs. The shuttle vectors were used to generate recombinant adenoviral plasmids, which were pooled to produce adenovirus AdR-simBC using the AdEasy system [41, 43, 56–58]. The resultant adenoviral vector also expresses monomeric RFP. Knockdown efficiency was assessed by qPCR and functional assays of β-catenin signalling.

Construction of recombinant adenoviruses expressing Wnt3A, BMP-9, β-catenin*, DKK1, FrzB, Runx2, sLRP-5 and sLRP-6

Adenoviruses expressing Wnt3A, BMP-9, β-catenin*, DKK1, Runx2 and FrzB were generated previously using the AdEasy system [15–17, 41, 43, 57, 58]. In order to generate adenoviral vectors expressing sLRP-5 and sLRP-6, the extracellular domains of human LRP-5 and LRP-6 were PCR amplified and cloned into a shuttle vector pAdTrace-TO4, and subsequently used to generate adenoviral recombinants AdR-sLRP-5 and AdR-sLRP-6, respectively. Adenoviruses were produced and amplified in HEK293 cells. AdWnt3A, AdBMP-9, Adβ-catenin*, AdDKK1 and AdFrzB also express GFP, whereas AdR-Runx2, AdR-sLRP-5 and AdR-sLRP-6 express RFP as a marker for monitoring infection efficiency. Analogous adenoviruses expressing only GFP (AdGFP) and RFP (AdRFP) were used as controls [16, 17, 41, 43, 57, 58].

Preparation of conditioned medium

BMP-9 and Wnt3A conditioned media were prepared as described [59]. Briefly, subconfluent HCT116 cells (in 75-cm^2 flaks) were infected with an optimal titre of AdBMP-9, AdWnt3A or AdGFP control. At 15 hrs after infection, the culture medium was changed to serum-free DMEM. Conditioned medium was collected at 48 hrs after infection and used immediately.

ALP assays

ALP activity was assessed by colorimetric assay (using p-nitrophenyl phosphate as a substrate) and/or histochemical staining assay (using a mixture of 0.1 mg/ml napthol AS-MX phosphate and 0.6 mg/ml Fast Blue BB salt) as described [12, 13, 15–17].

Mineralization assay

C3H10T1/2 cells and MEFs were seeded in 24-well cell culture plates and infected with AdBMP-9 and AdR-simBC or AdFrzB. Infected cells were cultured in the presence of ascorbic acid (50 μg/ml) and β-glycerophosphate (10 mM). At 14 and 21 days after infection, mineralized matrix nodules were stained for calcium precipitation by means of Alizarin Red S staining, as described previously [6, 12, 13, 17, 60]. Cells were fixed with 0.05% (v/v) glutaraldehyde at room temperature for 10 min. After being washed with distilled water, fixed cells were incubated with 0.4% Alizarin Red S (Sigma-Aldrich) for 5 min., followed by extensive washing with distilled water. The staining of calcium mineral deposits was recorded under bright field microscopy.

Luciferase assay

Cells were seeded in 25-cm^2 flasks and transfected with 2 μg per flask of β-catenin/Tcf4-responsive luciferase reporter, pTOP-Luc [27, 41, 43, 61, 62] or Runx2-binding sites (OSE2)-luciferase reporter, p6OSE2-Luc [63] using LipofectAmine (Invitrogen, Carlsbad, CA, USA). At 16 hrs after transfection, cells were replated to 24-well plates. For Top-Luc reporter assay, cells were infected with AdWnt3a and AdRsimBC or AdFrzB, AdDKK1, AdRsLRP-5, AdRsLRP-6 at 4 hrs after replating. For p6OSE2-luc reporter assay, cells were infected with Adβ-catenin* and AdBMP-9 or AdR-Runx2 at 4 hrs after replating. At 24 to 48 hrs after infection, cells were lysed and cell lysates were collected for luciferase assays using Promega's Luciferase Assay Kit (Promega, Madison, WI, USA). Each assay condition was performed in triplicate.

RNA isolation and quantitative real-time PCR (qPCR) analysis

Total RNA was isolated using TRIZOL Reagents (Invitrogen). qPCR was carried out as described [15–17]. Total RNA was used to generate cDNA templates by RT reaction with hexamer and Superscript II RT (Invitrogen). The first strand cDNA products were further diluted 5- to 10-fold and used as qPCR templates. qPCR primers (Supporting Table 1) were 18-mers, designed with the Primer3 program to amplify the gene of interest (approximately 120 bp). SYBR Green-based qPCR analysis was carried out using the Opticon DNA Engine thermocycler (M J Research, Waltham, MA, USA). The pUC19 was used as a standard. Duplicate reactions were carried out for each sample, and all samples were normalized by the expression level of GAPDH.

Immunofluorescence staining

Immunofluorescence staining was carried out as described [15–17]. Briefly, cells were fixed with methanol at –20 °C for 15 min. and washed with PBS. The fixed cells were permeabilized with 1% NP-40 and blocked with 10% goat serum, followed by incubation with a β-catenin antibody (Santa Cruz Biotechnology, Santa Cruz, CA, USA) for 60 min. After washing, cells were incubated with biotin-labelled secondary antibody for 30 min., followed by incubating cells with streptavidin-Alexa Fluor 488 or streptavidin-Alexa Fluor 568 (Molecular Probes, Eugene, OR, USA) for 20 min. at room temperature. The presence of β-catenin protein was examined under a fluorescence microscope. Stains without the primary antibody, or with control IgG, were used as negative controls.

ChIP assay

ChIP was carried out as described previously [17]. Briefly, 5×10^6 cells were used for each ChIP assay, and each assay condition was done in duplicate. Subconfluent C3H10T1/2 cells were infected with AdBMP-9, Adβ-catenin* or AdGFP for 36 hrs. Cells were cross-linked with 1% formaldehyde in PBS at room temperature for 10 min. Cross-linking was terminated by adding 1.0 M glycine to a final concentration of 125 mM at room temperature for 10 min. Cells were washed with ice-cold PBS twice and scraped into ice-cold PBS containing proteinase inhibitors (Roche, Indianapolis, IN, USA). Cells were collected and resuspended in lysis buffer (50 mM HEPES/KOH pH 7.5, 150 mM NaCl, 1 mM EDTA, 1% Triton X-100, 0.1% SDS and 0.1% sodium deoxycholate) containing protease inhibitors. The lysate was subjected to sonication to shear chromatin to 500 to 1000 bp fragments. One-third of the lysate was incubated with 5 M NaCl at 65°C to reverse the cross-linking, phenol-chloroform extracted, ethanol precipitated and kept at –80°C as an input control for PCR analysis. The remaining two-thirds of the lysate were subjected to immunoprecipitation using β-catenin antibody, Runx2 antibody (Santa Cruz Biotechnology) or mouse IgG (PIERCE Biotechnology, Rockford, IL, USA). Immunoprecipitated complexes were collected by protein G sepharose beads. Precipitants were sequentially washed with lysis buffer twice, followed by an additional wash with wash buffer (lysis buffer with

0.5 M NaCl). After the final wash, 200 μl of elution buffer (50 mM Tris-HCl, 10 mM EDTA, pH 7.5, 1% SDS) was added, and beads were rotated at room temperature for 15 min. Then 5 M NaCl was added to reverse the formaldehyde cross-linking. The DNA was extracted with phenol/chloroform, ethanol precipitated and resuspended in ddH_2O for PCR analysis. Two pairs of primers specific for mouse osteocalcin promoter were used for PCR amplification (Supporting Table 1): Primer set CP-1 (located at −0.5 kb relative to the transcription start site of osteocalcin mRNA): 5′-GCA GAA GTT GAT GTT GAA GCT ATA G-3′ and 5′-CAA TTG AGA AAA TGC CTC CAT AAG -3′; Primer set CP-2 (located at −1.0 kb): 5′-CAT TTC CAC CTA GAG CAA GTG AC-3′ and 5′-CAT TAA GCT CCA GAT GCC TGG GAC-3′. The expected products were resolved on 1.5% agarose gels.

Stem cell implantation

The use and care of animals was approved by the Institutional Animal Care and Use Committee. C3H10T1/2 or MEFs were infected with AdBMPs, AdRFP and AdR-simBC or AdFrzB for 15 hrs, and collected for subcutaneous injection (5×10^6/injection) into the flanks of athymic nude (nu/nu) mice (five animals per group, 4–6-week old, male, Harlan Sprague Dawley). At 5 weeks after implantation, animals were killed, and the implantation sites were retrieved for microCT analysis, histological evaluation and other stains.

Histological evaluation

Retrieved tissues were decalcified, fixed in 10% formalin, and embedded in paraffin. Serial sections of the embedded specimens were stained with haematoxylin and eosin. Masson's Trichrome stain was carried out as described [13].

MicroCT analysis

The cone-beam micro-CT system used for acquiring mouse data consists of a microfocal X-ray source, an orthogonally mounted rotary stage with object holder, and a CsI-coupled CMOS detector. The microfocal X-ray source (MX-20, Faxitron, IL, USA) is comprised a tungsten anode with beryllium exit window, has a focal spot of 20 μm, and was operated at 28 KeV. The 14-bit digital camera (Bioptics, Tucson, AZ, USA) includes a CsI scintillator plate and a 2048 × 1024 array of CMOS thin-film transistors and photodiodes with a pixel size of 50 μm. The back projection-filtration algorithm with a unit appodization function was used for reconstructing volumetric images from the acquired cone-beam data. Volume-rendered views were generated with opacity-weighted compositing and gradient-based shading (VolView 2.0: Kitware, Inc., Clifton Park, NY, USA) techniques.

Results

Canonical Wnt3A acts synergistically on BMP-9-induced osteogenic differentiation of MSCs

Although the exact mechanisms remain to be fully delineated, both Wnt and BMP signalling pathways are shown to regulate the proliferation and differentiation processes of MSCs [7]. As shown in Fig. 1A, overexpression of either canonical Wnt3A or BMP-9 was shown to effectively induce ALP activity in mesenchymal C3H10T1/2 cells. We previously demonstrated that, among the 14 types of BMPs, BMP-9 is one of the most osteogenic BMPs, and yet is one of the least studied [5, 6, 12, 13, 27, 60]. Through microarray expression profiling, we demonstrated that Wnt3A and BMP-9 regulate a set of mutual target genes, such as CTGF/CCN2, in MSCs [6, 16, 17]. Nonetheless, it is conceivable that a distinct set of downstream mediators is required for either Wnt3A or BMP-9 induced osteogenic differentiation. As shown in Fig. 1B and C, a detailed time-course experiment revealed that Wnt3A induced a stronger and earlier ALP activity than that of BMP-9. At day 3, Wnt3A-induced ALP activity is approximately threefold the ALP activity of BMP-9. Wnt3A induced ALP activity peaked at day 6 (Fig. 1B), whereas BMP-9-induced ALP activity peaked at day 8 (Fig. 1C). Wnt3A was shown to enhance BMP-9-induced ALP activity (Fig. 1D), or *vice versa* (Fig. 1E), although the synergistic effects decreased significantly at late time-points (*i.e.* day 10). These results suggest that there may be crosstalk between the two pathways.

FrzB (and DKK1, to a lesser extent) inhibits BMP-9-induced osteogenic differentiation of MSCs and MEFs

We sought to determine the effects of Wnt signalling inhibitors on BMP-9-induced osteogenic differentiation. To effectively introduce Wnt antagonists FrzB and DKK1 into MSCs, we previously constructed recombinant adenoviral vectors expressing FrzB or DKK1, along with the expression of a GFP marker [6, 16, 17]. We also constructed two adenoviral vectors that express the extracellular domains of human LRP-5 and LRP-6, namely sLRP-5 and sLRP-6, respectively, along with the expression of a RFP marker. The four adenoviral vectors were shown to effectively transduce C3H10T1/2 progenitor cells (Fig. 2A, left panel), and resulted in an apparent decrease of Wnt3A-induced β-catenin accumulation in C3H10T1/2 cells (Fig. 2A, right panel). Furthermore, overexpression of the four inhibitors was shown to inhibit the Wnt3A-induced β-catenin/Tcf4 reporter activity in a dose-dependent manner (Fig. 2B). These results demonstrated that adenovirus-mediated expression of DKK1, FrzB, sLRP-5 or sLRP-6 effectively inhibits canonical Wnt/β-catenin activity.

We next tested the effect of the four Wnt inhibitors on BMP-9-induced osteogenic differentiation. As shown in Fig. 2C, overexpression of FrzB resulted in an approximately 90% decrease in BMP-9-induced ALP activity in C3H10T1/2 cells at both time-points tested. DKK1 overexpression led to a 40% decrease in BMP-9-induced ALP activity at day 7, while the inhibitory effect on ALP activity was less obvious at day 10. Interestingly, overexpression of sLRP-5 or sLRP-6 in C3H10T1/2 cells was reproducibly shown to slightly enhance BMP-9-induced ALP activity, yet the mechanism is not understood. The inhibitory effects of FrzB and DKK1 were further confirmed in pluripotent MEFs, which are used as a common

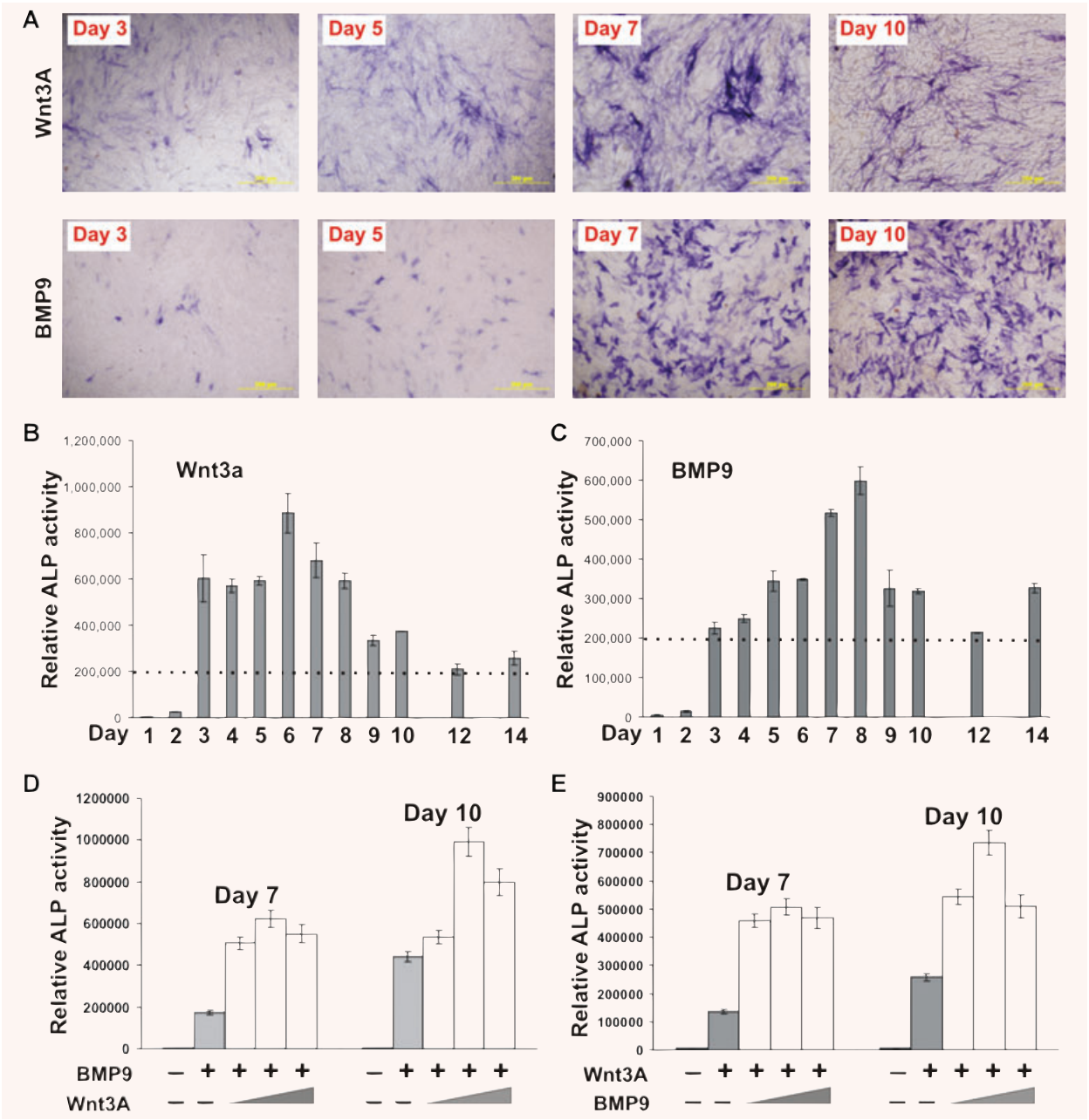

Fig. 1 Synergistic effect of canonical Wnt and BMP-9 on osteogenic differentiation of mesenchymal stem cells (MSCs). (**A**) Early osteogenic marker alkaline phosphatase (ALP) is induced by Wnt3A or BMP-9. MSC line C3H10T1/2 cells were infected with a comparable titre of AdWnt3A, AdBMP-9 or AdGFP control (not shown). ALP activity was detected histochemically at the indicated time-points. (**B**) and (**C**) Time-course comparison between Wnt3A and BMP-9-induced ALP activity in MSCs. C3H10T1/2 cells were infected with a comparable titre (MOI = 30 pfu/cell) of AdWnt3A, AdBMP-9 or AdGFP control (not shown). ALP activity was quantitatively assessed using a colorimetric assay (see 'Materials and methods') at the indicated time-points. The dotted lines indicate the same level of relative ALP activity. (**D**) and (**E**) Synergistic effects between Wnt3A and BMP-9 on osteogenic differentiation in MSCs. C3H10T1/2 cells were infected with AdBMP-9 or AdGFP (MOI = 10 pfu/cell) and various concentrations of Wnt3A conditioned medium (**D**), or infected with AdWnt3A or AdGFP (MOI = 10 pfu/cell) and various concentrations of BMP-9 conditioned medium (**E**). ALP activities were quantitatively assessed at the indicated time-points. Data are present as mean ± S.D. All ALP assays were carried out in triplicate, and confirmed in at least two independent experiments.

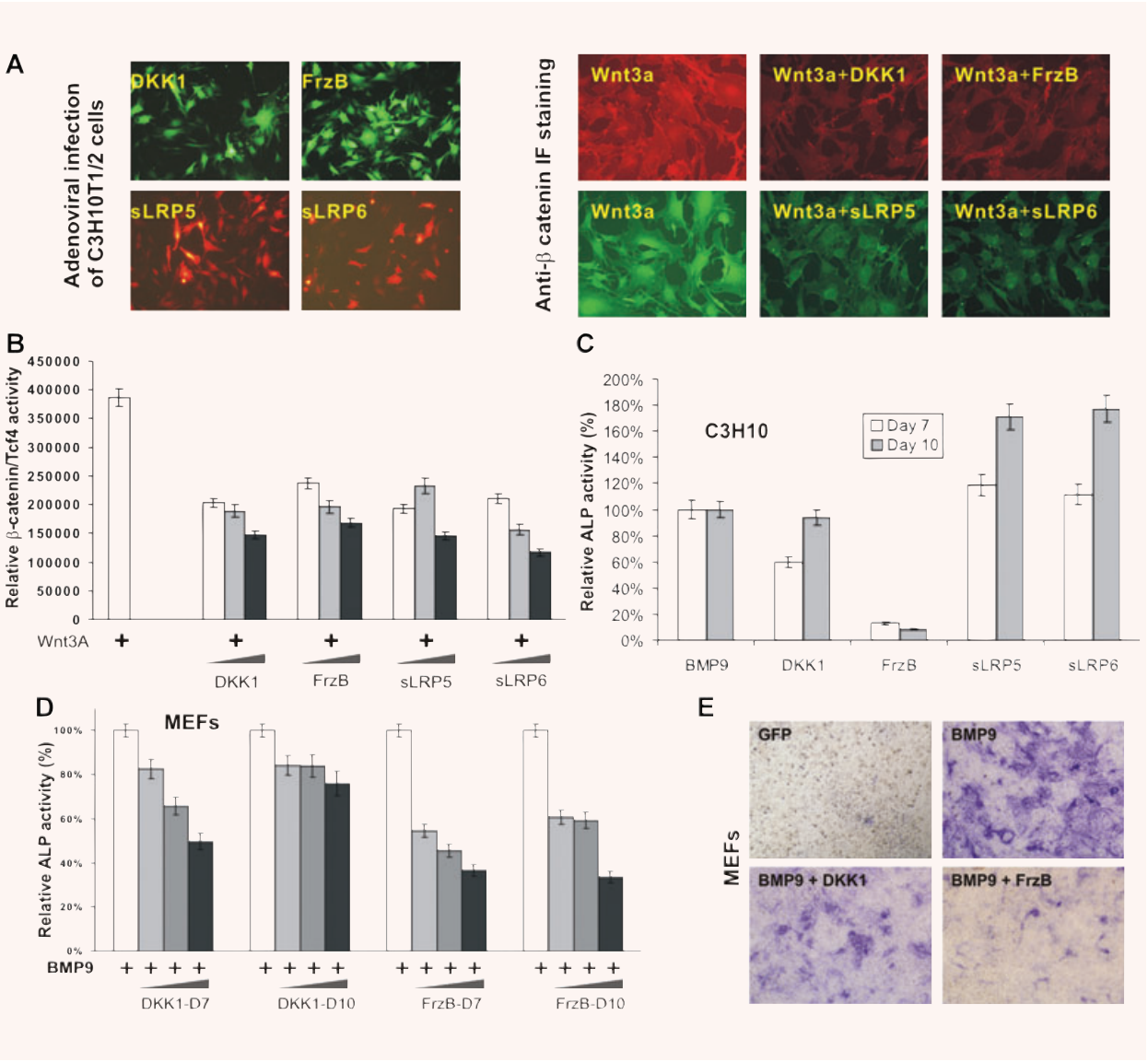

Fig. 2 Wnt antagonists inhibit BMP-9-induced osteogenic differentiation of MSCs and mouse embryonic fibroblasts (MEFs). (**A**) Effective transduction of C3H10T1/2 cells by adenoviral vectors expressing the Wnt signalling inhibitors DKK1, FrzB, sLRP-5 and sLRP-6. Left part: Subconfluent C3H10T1/2 cells were infected with a comparable titre of the four adenoviruses. At 36 hrs, infected cells were examined under a fluorescence microscope for GFP (Dkk1 and FrzB) or RFP (sLRP-5 and sLRP-6) expression. Right part: Subconfluent C3H10T1/2 cells were infected with the four Wnt inhibitor adenoviruses for 24 hrs, and stimulated with Wnt3A conditioned medium for another 12 hrs. Cells were fixed and subjected to immunofluorescence staining using an anti-β-catenin antibody. AdGFP infection and control IgG were used as controls. (**B**) Functional verification of adenoviral vectors expressing Wnt inhibitors. C3H10T1/2 cells were transfected with the Tcf4/LEF1 reporter TOP-Luc and infected with increasing amounts of AdDkk1, AdFrzB, AdR-sLRP-5 and AdR-sLRP-6, along with AdWnt3A. At 36 hrs, cells were collected for luciferase assays. Data are present as mean ± S.D. (**C**) Effect of the Wnt inhibitors on BMP-9-induced alkaline phosphatase (ALP) activity in MSCs. C3H10T1/2 cells were con-infected with AdBMP-9 and AdGFP, AdDkk1, AdFrzB, AdR-sLRP-5 or AdR-sLRP-6. ALP activities were quantitatively assessed at the indicated time-points. Data are present as mean ± S.D. (**D**) and (**E**) Effect of Dkk1 and FrzB on BMP-9-induced ALP activity in MEFs. Primary MEFs were co-infected with AdBMP-9 and AdGFP, or increasing titres of AdDkk1 or AdFrzB. ALP activities were quantitatively assessed at day 7 (Dkk1-D7 and FrzB-D7) and day 10 (Dkk1-D10 and FrzB-D10). Data are present as mean ± S.D. Histochemical staining of ALP activity (**E**) was done at 10 days after infection.

source of MSCs [55]. As illustrated in Fig. 2D, overexpression of FrzB or DKK1 was shown to inhibit BMP-9-induced ALP activity in MEFs in a dose-dependent manner. Consistent with the results observed in Fig. 2C, FrzB was a more potent inhibitor than DKK1 (Fig. 2D), which was also confirmed by the histochemical staining assay of ALP activity (Fig. 2E). Overexpression of sLRP-5 or sLRP-6 did not inhibit BMP-9-induced ALP activity (Supporting Fig. S1A). Taken together, these results suggest that FrzB may be a potent inhibitor of BMP-9-induced osteogenic differentiation. DKK1 antagonizes Wnt signalling by inhibiting Wnt interaction with LRP-5/6 co-receptors [27, 40, 62, 64]. Based on these results in which DKK1 weakly inhibited (and sLRP-5/sLRP-6 failed to inhibit) BMP-9-induced ALP activity, Wnt co-receptors LRP-5/6 may play a limited role in BMP-9-induced osteogenic differentiation of MSCs.

Stabilized β-catenin enhances BMP-9-induced ALP activity in MSCs

β-Catenin is considered as the essential signalling mediator of the canonical Wnt pathway [27, 34, 40, 62, 64]. We examined whether overexpression of the stabilized β-catenin exerted any effects on BMP-9-induced osteogenic differentiation. We previously constructed a recombinant adenoviral vector that expresses a stabilized form (S33Y) of human β-catenin [17, 61, 65]. Overexpression of the stabilized β-catenin alone in C3H10T1/2 resulted in a weak but detectable increase in ALP activity (Fig. 3A, top row). However, BMP-9-induced ALP activity was drastically enhanced by the overexpression of the stabilized β-catenin (Fig. 3A, bottom row). A quantitative analysis of BMP-9-induced ALP activity further confirmed that β-catenin can potentiate BMP-9-induced osteogenic differentiation of MSCs in a dose-dependent manner (Fig. 3B).

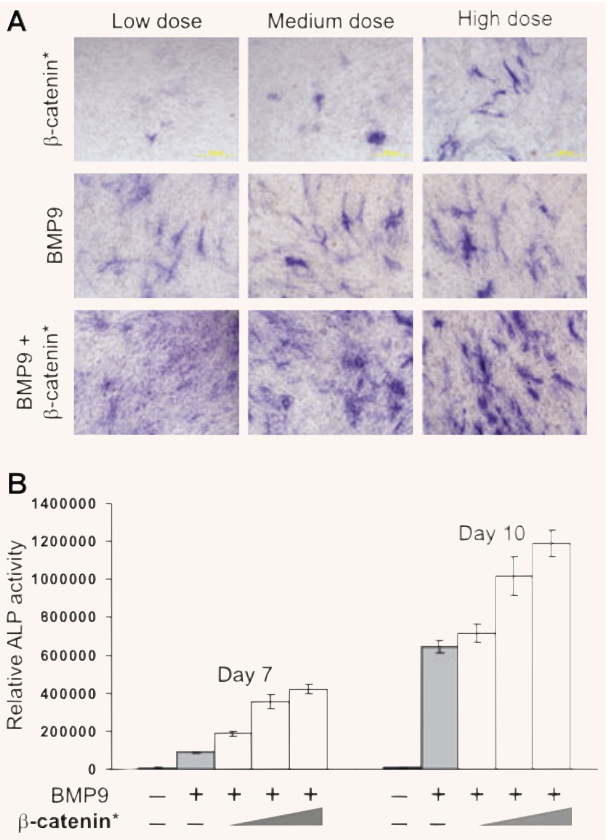

Fig. 3 Overexpression of a stabilized β-catenin enhances BMP-9-induced alkaline phosphatase (ALP) activity in MSCs. (**A**) Qualitative assessment of β-catenin-mediated augmentation of BMP-9-induced ALP activity. C3H10T1/2 cells were infected with varying titres of Adβ-Cat* and/or AdBMP-9. ALP activities were histochemically stained at 10 days after infection. (**B**) Quantitative assessment of β-catenin-mediated enhancement of BMP-9-induced ALP activity. C3H10T1/2 cells were co-infected with a fixed titre of AdBMP-9 and varying titres of Adβ-Cat*. ALP activities were quantitatively assessed at the indicated time-points. Data are present as mean ± S.D.

Knockdown of β-catenin expression inhibits BMP-9-induced ALP activity in MSCs

We next sought to determine the importance of β-catenin in BMP-9-induced osteogenic differentiation by silencing β-catenin expression in MSCs. Using our recently developed pSOS system [56], we selected and validated three siRNA sites targeting the coding region of mouse β-catenin (Fig. 4A). An adenovirus pool that expresses all three siRNA sites was then generated. The resultant AdR-simBC, which also expresses RFP marker, was shown to effectively transduce C3H10T1/2 progenitor cells (Fig. 4A). AdR-simBC was shown to inhibit Wnt3A conditioned medium-induced nuclear accumulation of β-catenin protein (Fig. 4A), as well as to inhibit Wnt3A-induced β-catenin/Tcf4 transcriptional activation in a dose-dependent manner (Fig. 4B). These results demonstrated that silencing β-catenin expression was achieved by adenovirus-mediated expression of β-catenin siRNAs.

We subsequently examined the effect of β-catenin knockdown on osteogenic differentiation induced by Wnt3A or BMP-9. As shown in Fig. 4C, silencing β-catenin expression in C3H10T1/2 cells inhibited Wnt3A-induced ALP activity in a dose-dependent manner, and the inhibitory effect on ALP activity was more pronounced at day 7, suggesting that β-catenin may play an important role in mediating canonical Wnt-induced early stage of osteogenic differentiation. When β-catenin expression was silenced in C3H10T1/2 cells, BMP-9-induced ALP activity was drastically inhibited in a dose-dependent manner (Fig. 4D, and Supporting Fig. S1B). A similar inhibitory effect of β-catenin knockdown on BMP-9-induced ALP activity was observed in MEF cells (Fig. 4E). These results strongly suggest that β-catenin may play an important role in regulating BMP-9-induced early stage of osteogenic differentiation of MSCs.

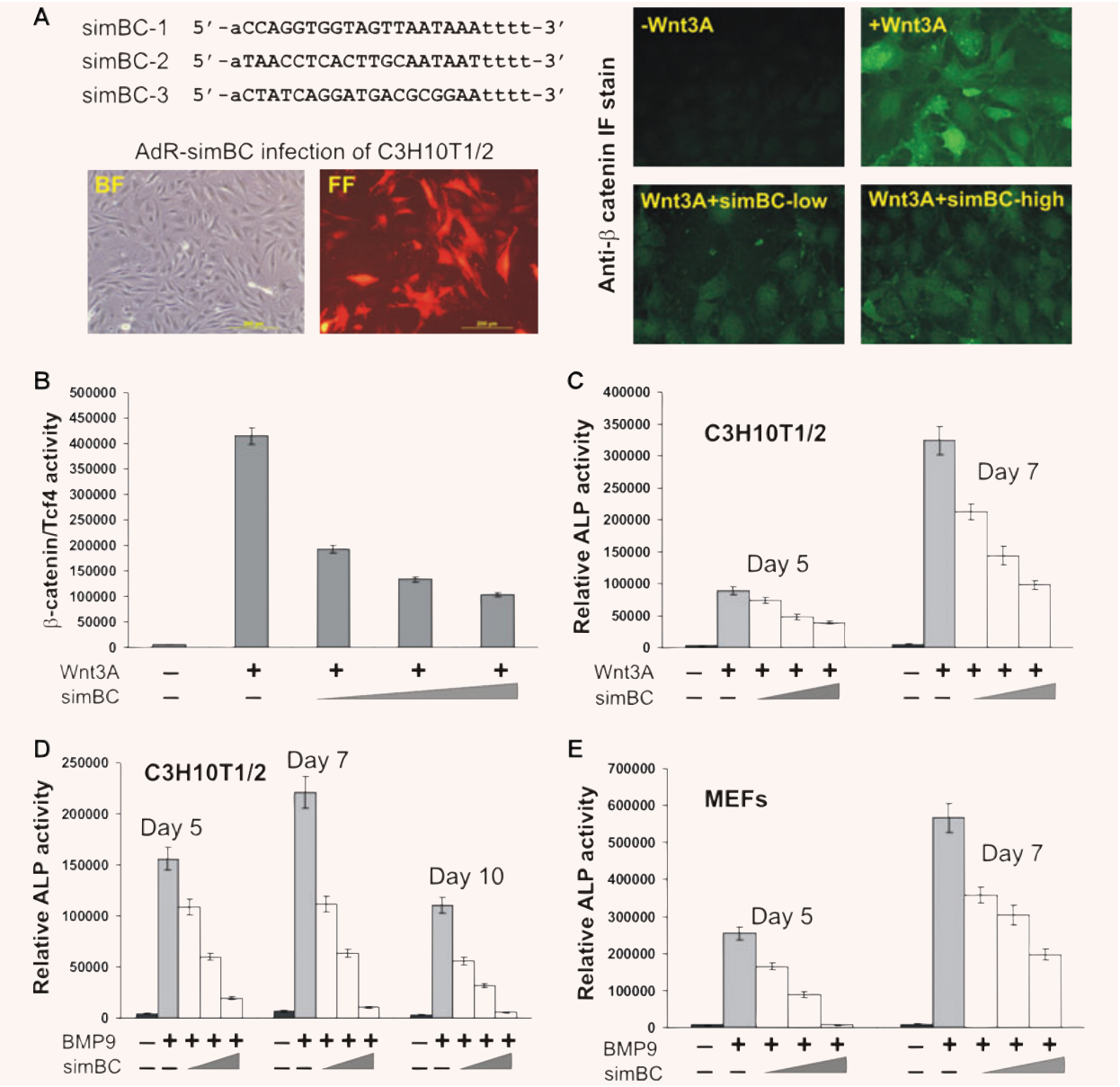

Fig. 4 Knockdown of β-catenin inhibits BMP-9-induced early osteogenic marker alkaline phosphatase (ALP) activity in MSCs and mouse embryonic fibroblasts (MEFs). (**A**) Construction and verification of siRNAs targeting mouse β-catenin expression, simBC. The three listed candidate siRNA sites were validated using our recently developed pSOS system and subcloned into an adenoviral shuttle vector. The resultant adenovirus AdR-simBC, which also expresses RFP, was used to infect C3H10T1/2 cells. The infection efficiency was assessed under a fluorescence microscope. With immunofluorescence stain using an anti-β-catenin antibody, AdR-simBC effectively knocked down Wnt3A-induced β-catenin accumulation in C3H10T1/2 cells. BF, bright field. (**B**) AdR-simBC effectively inhibits Tcf4/LEF1 reporter activity. C3H10T1/2 cells were transfected with TOP-Luc reporter and infected with varying titres of AdR-simBC, in the presence or absence of Wnt3A conditioned medium. At 36 hrs, cells were collected for luciferase assay. (**C**) Silencing of β-catenin inhibits Wnt3A-induced ALP activity in MSCs. C3H10T1/2 cells were infected with varying titres of AdR-simBC, in the presence or absence of Wnt3A conditioned medium. ALP activities were quantitatively assessed at the indicated time-points. (**D**) Silencing of β-catenin inhibits BMP-9-induced ALP activity in MSCs. C3H10T1/2 cells were infected with varying titres of AdR-simBC, in the presence or absence of BMP-9 conditioned medium. ALP activities were quantitatively assessed at the indicated time-points. (**E**) Silencing of β-catenin inhibits BMP-9-induced ALP activity in MEFs. Primary MEFs were infected with varying titres of AdR-simBC, in the presence or absence of BMP-9 conditioned medium. ALP activities were quantitatively assessed at the indicated time-points. All data are present as mean ± S.D.

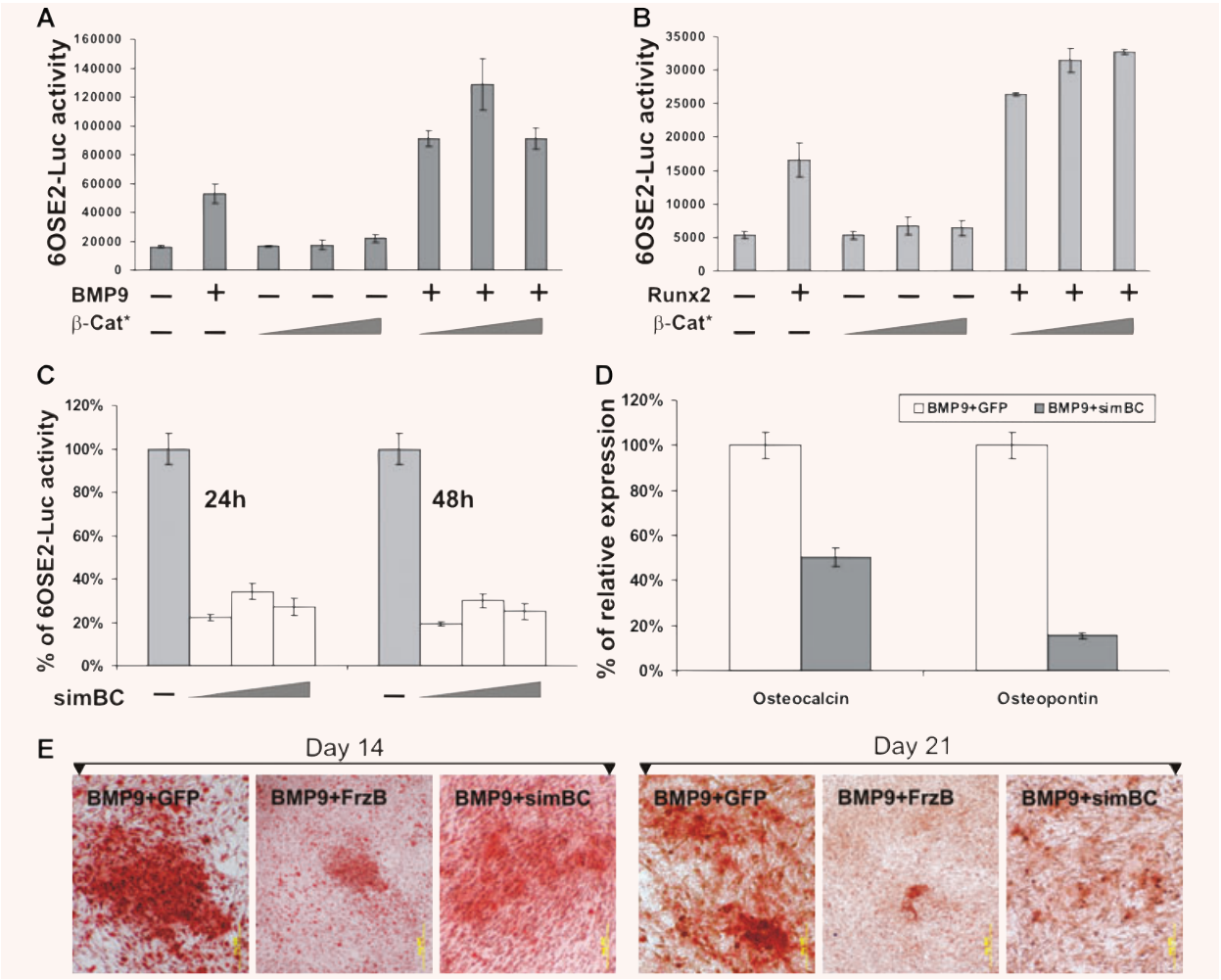

Fig. 5 β-Catenin also plays an important role in BMP-9-induced late stage of osteogenic differentiation. (**A**) Synergistic effect between β-catenin and BMP-9 on osteocalcin promoter reporter. C3H10T1/2 cells were transfected with p6OSE2-Luc reporter and infected with varying titres of Adβ-Cat*, in the presence or absence of BMP-9 conditioned medium. At 48 hrs, cells were collected for luciferase assay. Data are present as mean ± S.D. (**B**) Synergistic effect between β-catenin and Runx2 on osteocalcin promoter reporter. C3H10T1/2 cells were transfected with p6OSE2-Luc reporter and co-infected with varying titres of Adβ-Cat* and/or AdRunx2. At 48 hrs, cells were collected for luciferase assay. Data are present as mean ± S.D. (**C**) Knockdown of β-catenin inhibits BMP-9-induced activation of osteocalcin promoter reporter. C3H10T1/2 cells were transfected with p6OSE2-Luc and infected with varying titres of AdR-simBC in the presence of BMP-9 conditioned medium. Cells were collected for luciferase at the indicated time-points. (**D**) Knockdown of β-catenin inhibits BMP-9-induced expression of late osteogenic markers. C3H10T1/2 cells were co-infected with AdBMP-9 and AdR-simBC or AdGFP for 10 days. Total RNA was isolated for RT-PCR and qPCR analysis using primers specific for mouse osteocalcin and osteopontin. Experiments were done in triplicate. (**E**) Silencing of β-catenin and FrzB overexpression inhibit BMP-9-induced mineralization. C3H10T1/2 cells were co-infected with AdBMP-9 and AdFrzB, AdR-simBC, or AdGFP. At 14 and 21 days after infection, cells were fixed and subjected to Alizarin Red S staining. Representative images are shown (magnification, 40×).

β-Catenin plays an important role in the BMP-9-induced late stage differentiation of MSCs

Although ALP is a well-established early osteogenic marker, it is hardly an accurate predictor of the late stage of osteogenic differentiation and bone formation [6, 7, 12, 13]. Thus, we sought to determine whether β-catenin played any role in the BMP-9-induced late stage of osteogenic differentiation. Osteocalcin and osteopontin are well-characterized markers of late osteogenesis [6, 7, 12, 13]. Using a commonly used Runx2-regulated osteocalcin promoter reporter [63], we found that overexpression of the stabilized β-catenin enhanced BMP-9-induced reporter activity (Fig. 5A). Osteocalcin is a known target of the osteogenic regulator Runx2 [66, 67], and overexpression of the stabilized β-catenin acted synergistically on Runx2-induced osteocalcin reporter

activity (Fig. 5B). Conversely, silencing β-catenin expression resulted in a drastic decrease in BMP-9-stimulated osteocalcin promoter activity (Fig. 5C). Quantitative PCR further confirmed that knockdown of the β-catenin expression inhibited BMP-9-induced expression of the late osteogenic markers osteocalcin and osteopontin in C3H10T1/2 cells (Fig. 5D). Accordingly, either overexpression of FrzB or knockdown of β-catenin expression was shown to effectively inhibit BMP-9-induced expression of osteocalcin and osteopontin in MEF cells (Supporting Fig. S2A). Furthermore, we found that either overexpression of FrzB or knockdown of β-catenin expression effectively inhibited the BMP-9-induced *in vitro* mineralization in C3H10T1/2 cells (Fig. 5E) and in MEF cells (Supporting Fig. S2B). These findings suggest that canonical Wnt/β-catenin signalling may play an important role in regulating both early and late stages of BMP-9-induced osteogenic differentiation.

Silencing of β-catenin expression inhibits BMP-9-induced ectopic bone formation *in vivo*

The above *in vitro* data demonstrated that canonical Wnt/β-catenin signalling plays an important role in BMP-9-induced osteogenic differentiation of MSCs. We sought to confirm these findings *in vivo via* stem cell implantation experiments. To knockdown β-catenin expression in MSCs, we co-infected C3H10T1/2 cells with AdBMP-9 and different titres of AdR-simBC (or AdRFP as controls) for 15 hrs (Fig. 6A, top row). The infected cells were collected and injected subcutaneously into athymic mice. At 5 weeks after injection, animals were killed, and the injection sites were retrieved. The gross appearance of the retrieved samples indicated that silencing β-catenin expression inhibited the formation of ectopic bony masses in a dose-dependent fashion (Fig. 6A, bottom row). A similar, if not more marked, inhibitory effect on bone formation was also observed in the implantation experiments using the MEF cells transduced with AdBMP-9 and AdR-simBC (Fig. 6B). When the ectopic bone formation was quantitatively analysed using microCT (Fig. 6C), silencing β-catenin expression (at the high dose of AdR-simBC) inhibited bone formation by 80% in C3H10T1/2 cells and 94% in MEFs, respectively (Fig. 6D). Further, consistent with our *in vitro* results, FrzB effectively inhibited BMP-9-induced ectopic bone formation in the MEF cells (Supporting Fig. 2C and D).

Histological evaluation indicated that silencing β-catenin expression inhibited BMP-9-induced osteogenic differentiation and osteoblast maturation in MSCs. Specifically, silencing β-catenin expression led to a marked decrease in osteoblast activity and bone formation upon BMP-9 stimulation (Fig. 6E, parts b and d *versus* a and c). Trichrome stain indicated that, while the BMP-9 control samples exhibit abundantly fully ossified matrix, samples retrieved from AdR-simBC co-infected MSCs display only focal ossification and a significant amount of osteoid or cartilaginous collagen matrix (Fig. 6E, parts f and h *versus* e and g). The presence of cartilage matrix in the samples co-transduced with BMP-9 and simBC was further confirmed by Alcian Blue stain (Fig. 6E, parts j and l *versus* i and k). Histological analysis also indicated that FrzB overexpression inhibited BMP-9-mediated osteogenic differentiation and ossification (Supporting Fig. 3). These results further confirm that canonical Wnt/β-catenin signalling plays an important role in BMP-9-induced osteogenesis.

BMP-9 induces the recruitment of both Runx2 and β-catenin to osteocalcin promoter.

It has been reported that there is crosstalk between Wnt and TGF-β/BMP signalling pathways [7, 68–70]. We have demonstrated that β-catenin acts synergistically with BMP-9 or Runx2 on regulating osteocalcin promoter (Fig. 5A and B). It has been reported that Runx2 may physically interact with β-catenin and Tcf/Lef1 complex [71, 72]. We asked whether BMP-9 induced the recruitment of Runx2 and β-catenin to the osteocalcin promoter. As illustrated in Fig. 7A, mouse osteocalcin promoter region contains at least four putative Runx2 binding sites and one putative LEF1/Tcf4 binding site, most of which are located within the proximal 1 kb region of the promoter. To assess the *in vivo* promoter binding activity, we carried out ChIP assays using the C3H10T1/2 cells infected with AdBMP-9, Adβ-catenin* or AdGFP (Fig. 7B). The presence of osteocalcin promoter fragments in the immunoprecipitated complexes was determined by semi-quantitative PCR analysis using two pairs of primers (Fig. 7A). As expected, BMP-9 stimulation induced the Runx2 binding to osteocalcin promoter (Fig. 7C, first lane), while the basal Runx2 binding to osteocalcin promoter was undetectable (Fig. 7C, third lane). Interestingly, expression of the stabilized β-catenin also induced the Runx2 binding to osteocalcin promoter (Fig. 7C, second lane), suggesting that β-catenin may facilitate the recruitment of Runx2 to osteocalcin promoter. Reciprocal immunoprecipitation using an anti-β-catenin antibody further demonstrated that BMP-9 stimulation induced the recruitment of β-catenin/Tcf complex to osteocalcin promoter (Fig. 7D). These results were reproducible in at least three independent experiments, and the initial input for each ChIP assay was comparable (Fig. 7E). These results suggest that β-catenin may coordinate with Runx2 in BMP-9-regulated osteogenic signalling in pre-osteoblast progenitors.

Discussion

Here, we investigated whether canonical Wnt/β-catenin signalling plays an important role in BMP-9-induced osteogenic signalling. We found that Wnt3A and BMP-9 enhance each other's ability to induce ALP activity in MSCs and MEFs. Wnt inhibitor FrzB inhibits BMP-9-induced ALP most effectively. Silencing β-catenin diminishes the BMP-9-induced early stage of osteogenic differentiation. We further demonstrated that β-catenin enhances BMP-9 and Runx2-induced osteocalcin promoter-based reporter activity,

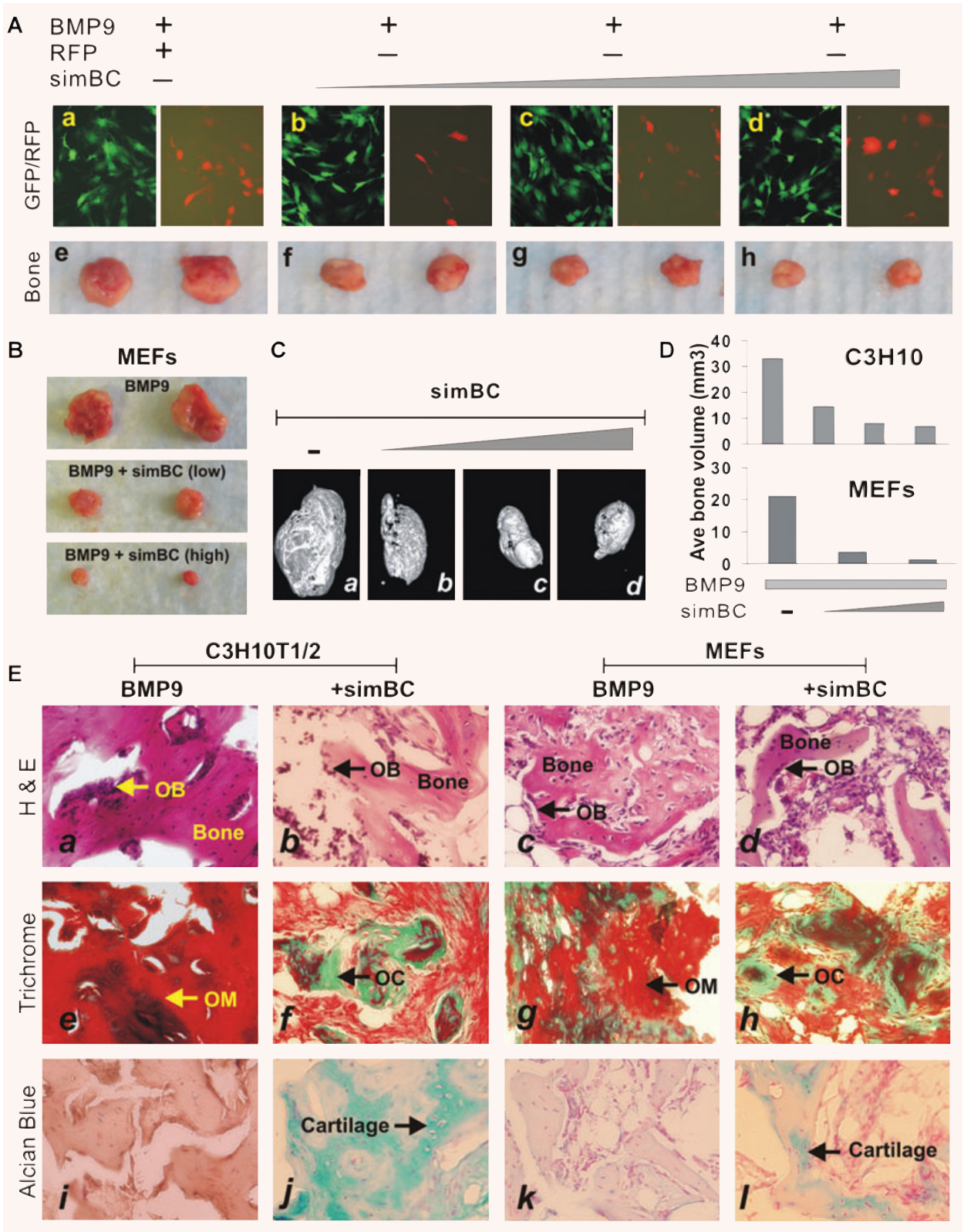

Fig. 6 Silencing of β-catenin expression inhibit BMP-9-induced ectopic bone formation in vivo. (**A**) Knockdown of β-catenin into C3H10T1/2 cells inhibits BMP-9-induced ectopic bone formation. C3H10T1/2 cells were co-infected with AdBMP-9 and varying titres of AdR-simBC, or AdRFP for 15 hrs, and the co-infection efficiency was examined under a fluorescence microscope. The infected cells were collected and subjected to subcutaneous injection into athymic mice. At 5 weeks after implantation, animals were killed and bony masses were retrieved. Representative gross images are shown (parts **e** to **h**). (**B**) BMP-9-induced bone formation in mouse embryonic fibroblasts (MEFs) is also inhibited by silencing β-catenin expression. A similar set of experiments as described in (**A**) was carried out in MEFs. (**C**) MicroCT analysis. The retrieved masses from (**A**) were further subjected to microCT scanning. Representative reconstructed 3-dimmensional images are shown. (**D**) Knockdown of β-catenin reduces the volume of BMP-9-induced bone formation. Bone volume (mm^3) was calculated based on microCT scanning data. The average bone volume of each group is shown. (**E**) The retrieved samples were decalcified and subjected to haematoxylin and eosin staining (parts **a** to **d**), Masson's Trichrome staining (parts **e** to **h**) and Alcian Blue staining (parts **i** to **l**). Representative images are shown. For the Trichrome stain, decalcified ossified matrix stained dark red, whereas osteoid or cartilage matrix stained blue. For the Alcian Blue stain, cartilage stained blue. OB, osteoblast; OC, osteoid or cartilage-like matrix; OM, ossified or mineralized matrix. Magnification, 150×.

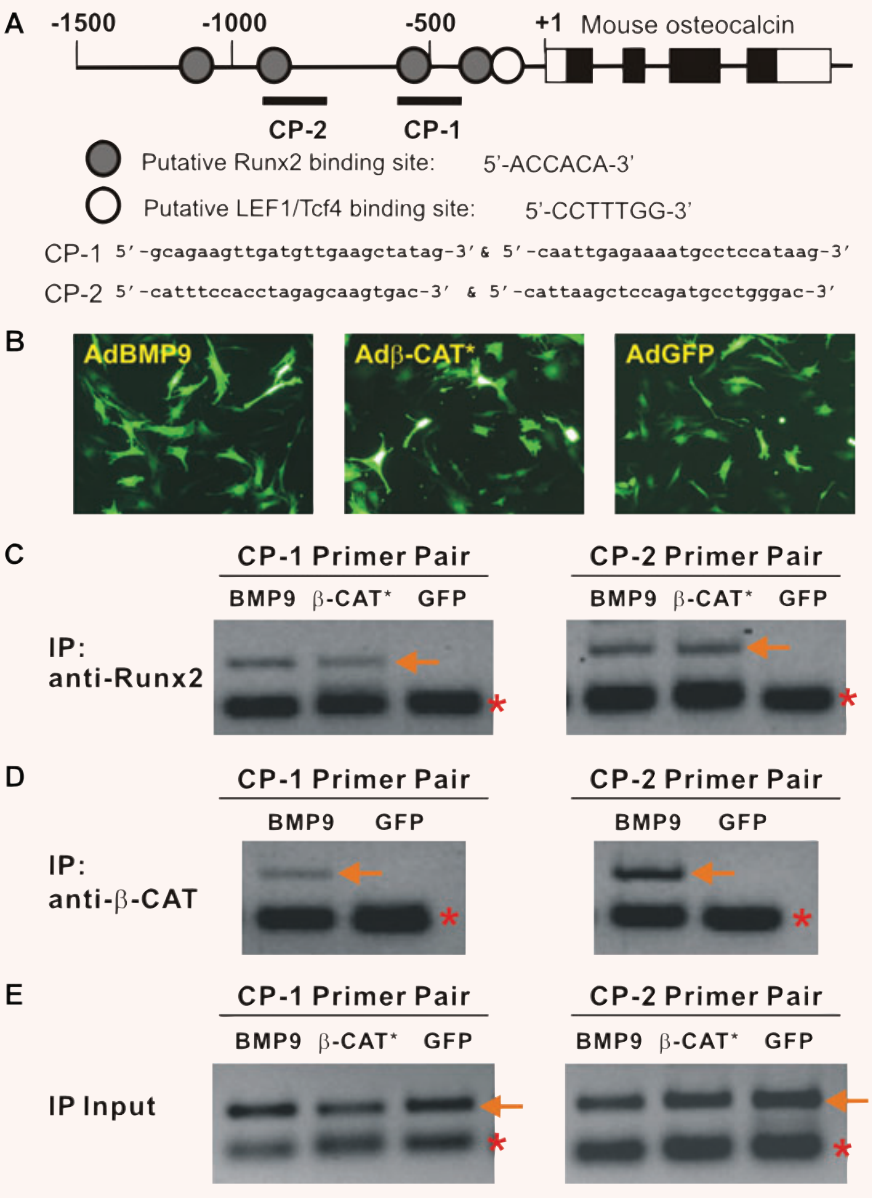

Fig 7. BMP-9-induced recruitment of both Runx2 and β-catenin to osteocalcin promoter. (**A**) Schematic features of the genomic arrangement of the mouse osteocalcin promoter. The boxed regions represent exons and the filled boxes represent the coding region. The filled circles represent putative Runx2 binding sites, while the open circle represents the putative LEF1/Tcf4 binding site. CP-1 and CP-2 are the PCR primer pairs used for chromatin immunoprecipitation (ChIP) analysis. (**B**) Efficient transduction of MSCs by AdBMP-9, AdβCat* and AdGFP for ChIP assay. Subconfluent C3H10T1/2 cells were infected with AdBMP-9, AdβCat* or AdGFP. Expression of GFP was examined at 36 hrs under a fluorescence microscope, immediately prior to ChIP analysis. (**C**) Both BMP-9 and β-catenin induce recruitment of Runx2 to OC promoter. The infected cells were cross-linked, sonicated and subjected to ChIP using a Runx2 antibody (Santa Cruz Biotechnology). The precipitated DNA-protein complexes were de-crosslinked and processed for PCR analyses using both pairs of primers listed in Fig. 7A. (**D**) BMP-9 induces recruitment of β-catenin to OC promoter. A similar ChIP procedure was carried out as described above, except that a β-catenin antibody was used for immunoprecipitation. (**E**) Equal amount of DNA-protein complex input was used for each ChIP sample. The arrows indicate the expected PCR products, while the asterisks denote the primer dimmers of PCR reactions. These results are representative of three independent experiments.

whereas silencing β-catenin leads to a decrease in BMP-9-induced expression of osteocalcin and osteopontin. Knockdown of β-catenin or overexpression of FrzB inhibits BMP-9-induced matrix mineralization *in vitro* and ectopic bone formation *in vivo*. ChIP analysis indicated that BMP-9 induces the recruitment of both Runx2 and β-catenin to the osteocalcin promoter.

Based on our findings, we propose a working model as illustrated in Fig. 8, which depicts that canonical Wnt signalling, through a cooperative interaction between β-catenin and Runx2, plays an important role in BMP-9-induced osteogenic differentiation of MSCs. As depicted in Fig. 8A, BMP-9 regulates Runx2 and subsequent downstream osteogenic factors (such as osteocalcin) with a low efficiency in the absence of canonical Wnt signal, the presence of Wnt antagonist FrzB, or silencing of β-catenin expression. In the presence of canonical Wnt signal β-catenin acts cooperatively with BMP-9-induced Runx2 to effectively regulate osteogenic factors (Fig. 8B). This model underscores an important role of canonical Wnt signalling in BMP-9-induced osteogenic differentiation of MSCs.

Our results are supported by several studies on BMP2 osteogenic signalling. BMP2 was shown to control ALP expression and osteoblast mineralization by a Wnt autocrine loop [73]. The β-catenin signalling is critical for BMP2 to induce ectopic bone formation [47, 74]. It was also shown that β-catenin induced MSC commitment to the osteogenic lineage. However, an N-terminus truncated, active β-catenin alone was not sufficient to induce osteogenic differentiation and bone formation, unless other stimulatory signals were present, in particular BMP2 [75]. Thus, β-catenin may function as an 'insufficient activator β' of osteogenic differentiation by sensitizing uncommitted precursors to respond to osteogenic cues, such as BMP-9. Consistent with this notion, we found that the exogenous expression of Wnt3A or β-catenin in MSCs failed to induce ectopic bone formation (Tang N. and He T.-C., unpublished studies).

We have recently compared potentially important downstream mediators of Wnt3A and BMP-9 induced osteogenic differentiation in MSCs through gene expression profiling, and found that Wnt3A and BMP-9 regulated the expression of overlapping but distinct sets of downstream target genes [16, 17], suggesting that there may be an important crosstalk between BMP and Wnt-induced osteogenic signalling pathways. Although the molecular mechanisms behind this crosstalk are largely undefined, it was reported that β-catenin and Lef1/Tcf can form a complex with Smad4 and/or Smad1 [69, 76–79]. It was also shown that Runx2 formed a complex with Lef1/Tcf4 and regulated downstream target genes [71, 72]. However, the signalling crosstalk may be more complicated, as Lef-1 was found to repress the osteocalcin promoter *via* interaction with Cbfa1/Runx2 [48, 52]; and it has recently been reported that canonical Wnt signalling promotes osteogenesis by directly stimulating Runx2 expression [80]. Thus, molecular mechanism underlying the crosstalk between BMP-9 and canonical Wnt/β-catenin needs to be further investigated.

The mechanism underlying the distinct roles of Wnt inhibitors in BMP-9 signalling remains to be defined. Disruption by Dkk1 allows for unphosphorlyated β-catenin to stimulate osteogenesis

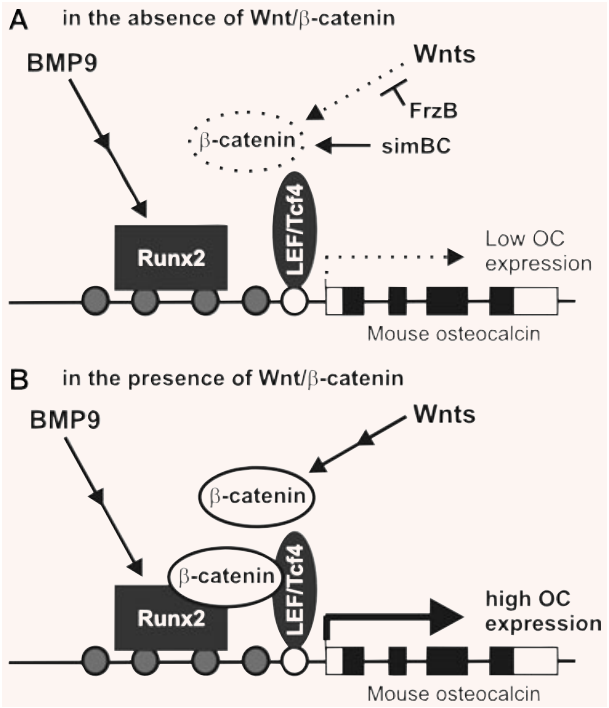

Fig. 8 A model depicting the mechanistic basis of β-catenin function in BMP-9-induced osteocalcin (OC) expression. (**A**) BMP-9 is less effective in inducing osteocalcin expression when the canonical Wnt/β-catenin signalling is inhibited by FrzB or silenced by β-catenin siRNA (*e.g.* simBC). (**B**) β-Catenin directly interacts with Runx2 and acts synergistically on regulating osteocalcin expression. The filled circles represent putative Runx2 binding sites, while the open circle represents the putative LEF1/Tcf4 binding site. The open and filled boxes represent the exons and the coding region of mouse osteocalcin gene, respectively.

[46], and bone mass is inversely proportional to Dkk1 levels in mice [81]. A recent study has also demonstrated that Dkk2 may play a role in late stages of osteoblast differentiation into mineralized matrix [82]. It has been shown that Wnt/β-catenin signalling in osteoblasts may coordinate postnatal bone acquisition by controlling the differentiation of both osteoblasts and osteoclasts [83], and by regulating osteoblast and chondrocyte differentiation during skeletogenesis [84–86]. We have found that overexpression of the LRP-5/6 inhibitor Dkk1 in MSCs did not significantly inhibit BMP-9-induced osteogenic differentiation. We conducted further analyses of LRP-5/6 in BMP-9 osteogenic signalling by overexpressing the secreted form of dominant-negative mutants of LRP-5 and LRP-6 [87], and found that neither sLRP-5 nor sLRP-6 was shown to effectively inhibit ALP activity induced by BMP-9 in MSCs. However, overexpression of the Fz receptor inhibitor FrzB effectively inhibited BMP-9-induced ALP activity and matrix mineralization *in vitro* and ectopic bone formation *in vivo*. Our results suggest that Wnt receptors and co-receptors may play distinct roles in BMP-9-induced osteogenic signalling.

Many Wnt Sfrps antagonists, including FrzB and Sfrp1, are highly expressed during the transition from pre-osteoblast to osteoblast [88]. *Sfrp1*$^{-/-}$ mice exhibit an increase in trabecular bone, but not cortical bone [80]. It was reported that although the *Lrp-5*$^{-/-}$ mice have a decrease in osteoblast numbers and bone formation rate, Wnt and Lef1-mediated signalling can still partially occur in *Lrp-5*$^{-/-}$ osteoblasts [89], suggesting Wnt signalling can be at least partially transduced *via* a LRP-5-independent mechanism. *Dkk1*$^{+/-}$ mice exhibit an increase in bone accrual and osteoblast numbers [90], while transgenic Dkk1 overexpression causes osteopenia and forelimb defects [91]. Our results were consistent with these *in vivo* studies, although the ineffective inhibition of BMP-9-mediated osteogenic differentiation may reflect the mechanistic differences of these inhibitors in skeletogenesis *versus* postnatal osteogenic differentiation. It has been recently reported that β-catenin signalling plays a disparate role in different phases of fracture repair [47], suggesting that Wnt/β-catenin may play a distinct role in skeletogenesis *versus* postnatal bone regeneration. Although the exact role of Wnt/β-catenin in BMP-9-induced osteogenic differentiation remains to be fully elucidated, our results demonstrate that canonical Wnt signalling, possibly through β-catenin interaction with Runx2, plays an important role in BMP-9-induced osteogenic differentiation of MSCs.

Acknowledgements

We thank Dr. Gerard Karsenty of Columbia University and Dr. Hiroyuki Kawashima of Niigata University Graduate School of Medical and Dental Sciences, Japan, for their kind provision of Cbaf1/Runx2 cDNA and p6OSE2-Luc reporter plasmids, respectively. This work was supported in part by research grants from China Natural Science Foundation and the Ministry of Science and Technology (J.L., B.C.H., M.T., L.C. and T.C.H.), the American Cancer Society (T.C.H. and H.H.L.), The Brinson Foundation (T.C.H.), the National Institutes of Health (R.C.H., T.C.H. and H.H.L.), and the Orthopaedic Research and Education Foundation (H.H.L.).

Supporting Information

Additional Supporting Information may be found in the online version of this article:

Supplemental Table 1
List of all oligonucleotide sequences used in the study.

Fig. S1 (**A**) BMP-9-induced alkaline phosphatase (ALP) activity is not affected by overexpression of sLRP-5 or sLRP-6 in mouse embryonic fibroblasts (MEFs). Subconfluent primary MEF cells were co-infected with AdBMP-9 and AdR-sLRP-5, AdR-sLRP-6, or AdGFP alone. At 10 days after infection, cells were subjected to histochemical staining of ALP activity. (**B**) BMP-9-induced ALP activity was inhibited as a result of silencing β-catenin expression. C3H101/2 cells were co-infected with AdBMP-9 and three different titres of AdR-simBC (or AdGFP or AdR-simBC alone). ALP activity was assessed histochemically at 7 days after infection.

Fig. S2 (**A**) Both FrzB and simBC inhibit BMP-9-induced expression of the late osteogenic markers osteocalcin and osteopontin. Mouse embryonic fibroblasts (MEFs) were co-infected with AdBMP-9 and AdR-simBC, AdFrzB, or AdGFP for 10 days. Total RNA was isolated for RT-PCR and qPCR analysis using primers specific for mouse osteocalcin and osteopontin. Experiments were done in triplicate. (**B**) Silencing of β-catenin and FrzB overexpression inhibit BMP-9-induced mineralization. C3H10T1/2 and MEF cells were co-infected with AdBMP-9 and AdFrzB, AdR-simBC, or AdGFP. At 21 days after infection, cells were fixed and subjected to Alizarin Red S staining. Representative macrographic images are shown. (**C**) and (**D**) FrzB overexpression inhibits BMP-9-induced ectopic bone formation. MEF cells were co-infected with AdBMP-9 and varying titres of AdFrzB, or AdGFP for 15 hrs and subjected to subcutaneous injection into athymic mice. At 5 weeks after implantation, animals were killed and bony masses were retrieved. Representative gross images are shown (**C**). The retrieved masses were further subjected to microCT scanning. Representative reconstructed 3-dimmensional images are shown (**D**).

Fig. S3 FrzB inhibits BMP-9-induced ectopic bone formation and mineralization. Mouse embryonic fibroblast (MEF) cells were co-infected with AdBMP-9 and AdFrzB (both low and high titres were used) or AdRFP for 15 hrs. The infected cells were collected and subjected to subcutaneous injection into athymic mice. At 5 weeks after implantation, animals were killed, and bony masses were retrieved, decalcified and subjected to haematoxylin and eosin staining (parts a to c), Masson's Trichrome staining (parts d to f) and Alcian Blue staining (parts g to i). Representative images are shown. For the Trichrome stain, decalcified ossified matrix stained dark red, whereas osteoid or cartilage matrix stained blue. For the Alcian Blue stain, cartilage stained blue. OC, osteoid or cartilage-like matrix; OM, ossified or mineralized matrix. Magnification, 150×.

This material is available as part of the online article from: http://www.blackwell-synergy.com/doi/abs/10.1111/j.1582-4934.2008.00569.x
(This link will take you to the article abstract).

Please note: Blackwell Publishing are not responsible for the content or functionality of any supporting materials supplied by the authors. Any queries (other than missing material) should be directed to the corresponding author for the article.

References

1. **Hogan BL.** Bone morphogenetic proteins: multifunctional regulators of vertebrate development. *Genes Dev*. 1996; 10: 1580–94.
2. **Ducy P, Karsenty G.** The family of bone morphogenetic proteins. *Kidney Int*. 2000; 57: 2207–14.
3. **Shi Y, Massague J.** Mechanisms of TGF-beta signaling from cell membrane to the nucleus. *Cell*. 2003; 113: 685–700.
4. **Attisano L, Wrana JL.** Signal transduction by the TGF-beta superfamily. *Science*. 2002; 296: 1646–7.
5. **Luo J, Sun MH, Kang Q, *et al.*** Gene therapy for bone regeneration. *Curr Gene Ther*. 2005; 5: 167–79.
6. **Luu HH, Song WX, Luo X, *et al.*** Distinct roles of bone morphogenetic proteins in osteogenic differentiation of mesenchymal stem cells. *J Orthop Res*. 2007; 25: 665–77.
7. **Deng ZL, Sharff KA, Tang N, *et al.*** Regulation of osteogenic differentiation during skeletal development. *Frontiers in Biosci*. 2008; 13: 2001–21.
8. **Song JJ, Celeste AJ, Kong FM, *et al.*** Bone morphogenetic protein-9 binds to liver cells and stimulates proliferation. *Endocrinology*. 1995; 136: 4293–7.
9. **Lopez-Coviella I, Berse B, Krauss R, *et al.*** Induction and maintenance of the neuronal cholinergic phenotype in the central nervous system by BMP-9. *Science*. 2000; 289: 313–6.
10. **Chen C, Grzegorzewski KJ, Barash S, *et al.*** An integrated functional genomics screening program reveals a role for BMP-9 in glucose homeostasis. *Nat Biotechnol*. 2003; 21: 294–301.
11. **Truksa J, Peng H, Lee P, *et al.*** Bone morphogenetic proteins 2, 4, and 9 stimulate murine hepcidin 1 expression independently of Hfe, transferrin receptor 2 (Tfr2), and IL-6. *Proc Natl Acad Sci USA*. 2006; 103: 10289–93.
12. **Cheng H, Jiang W, Phillips FM, *et al.*** Osteogenic activity of the fourteen types of human bone morphogenetic proteins (BMPs). *J Bone Joint Surg Am*. 2003; 85-A: 1544–52.
13. **Kang Q, Sun MH, Cheng H, *et al.*** Characterization of the distinct orthotopic bone-forming activity of 14 BMPs using recombinant adenovirus-mediated gene delivery. *Gene Ther*. 2004; 11: 1312–20.
14. **Peng Y, Kang Q, Cheng H, *et al.*** Transcriptional characterization of bone morphogenetic proteins (BMPs)-mediated osteogenic signaling. *J Cell Biochem*. 2003; 90: 1149–65.
15. **Peng Y, Kang Q, Luo Q, *et al.*** Inhibitor of DNA binding/differentiation helix-loop-helix proteins mediate bone morphogenetic protein-induced osteoblast differentiation of mesenchymal stem cells. *J Biol Chem*. 2004; 279: 32941–9.
16. **Luo Q, Kang Q, Si W, *et al.*** Connective tissue growth factor (CTGF) is regulated by Wnt and bone morphogenetic proteins signaling in osteoblast differentiation of mesenchymal stem cells. *J Biol Chem*. 2004; 279: 55958–68.
17. **Si W, Kang Q, Luu HH, *et al.*** CCN1/Cyr61 is regulated by the canonical Wnt signal and plays an important role in Wnt3A-induced osteoblast differentiation of mesenchymal stem cells. *Mol Cell Biol*. 2006; 26: 2955–64.
18. **Ducy P, Schinke T, Karsenty G.** The osteoblast: a sophisticated fibroblast under central surveillance. *Science*. 2000; 289: 1501–4.
19. **Prockop DJ.** Marrow stromal cells as stem cells for nonhematopoietic tissues. *Science*. 1997; 276: 71–4.
20. **Aubin JE.** Bone stem cells. *J Cell Biochem Suppl*. 1998; 31: 73–82.
21. **Pittenger MF, Mackay AM, Beck SC, *et al.*** Multilineage potential of adult human mesenchymal stem cells. *Science*. 1999; 284: 143–7.
22. **Caplan AI, Bruder SP.** Mesenchymal stem cells: building blocks for molecular medicine in the 21st century. *Trends in Mol Med*. 2001; 7: 259–64.
23. **Molofsky AV, Pardal R, Morrison SJ.** Diverse mechanisms regulate stem cell self-renewal. *Curr Opin Cell Biol*. 2004; 16: 700–7.
24. **Wang J, Wynshaw-Boris A.** The canonical Wnt pathway in early mammalian embryogenesis and stem cell maintenance/differentiation. *Curr Opin Genet Dev*. 2004; 14: 533–9.
25. **Kleber M, Sommer L.** Wnt signaling and the regulation of stem cell function. *Curr Opin Cell Biol*. 2004; 16: 681–7.
26. **Reya T, Clevers H.** Wnt signalling in stem cells and cancer. *Nature*. 2005; 434: 843–50.
27. **Luo J, Chen J, Deng ZL, *et al.*** Wnt signaling and human diseases: what are the therapeutic implications? *Lab Invest*. 2007; 87: 97–103.
28. **Karsenty G, Wagner EF.** Reaching a genetic and molecular understanding of skeletal development. *Dev Cell*. 2002; 2: 389–406.
29. **Varga AC, Wrana JL.** The disparate role of BMP in stem cell biology. *Oncogene*. 2005; 24: 5713–21.
30. **Zhang J, Li L.** BMP signaling and stem cell regulation. *Dev Biol*. 2005; 284: 1–11.
31. **Zhao GQ.** Consequences of knocking out BMP signaling in the mouse. *Genesis*. 2003; 35: 43–56.
32. **Urist MR.** Bone: formation by autoinduction. *Science*. 1965; 150: 893–9.
33. **Reddi AH.** Role of morphogenetic proteins in skeletal tissue engineering and regeneration. *Nat Biotechnol*. 1998; 16: 247–52.
34. **Cadigan KM, Nusse R.** Wnt signaling: a common theme in animal development. *Genes Dev*. 1997; 11: 3286–305.
35. **Glass DA, 2nd, Karsenty G.** *In vivo* analysis of Wnt signaling in bone. *Endocrinology*. 2007; 148: 2630–4.
36. **Bergwitz C, Wendlandt T, Kispert A, *et al.*** Wnts differentially regulate colony growth and differentiation of chondrogenic rat calvaria cells. *Biochim Biophys Acta*. 2001; 1538: 129–40.
37. **Fischer L, Boland G, Tuan RS.** Wnt signaling during BMP-2 stimulation of mesenchymal chondrogenesis. *J Cell Biochem*. 2002; 84: 816–31.
38. **Glass DA, 2nd, Karsenty G.** Molecular bases of the regulation of bone remodeling by the canonical Wnt signaling pathway. *Curr Top Dev Biol*. 2006; 73: 43–84.
39. **Wodarz A, Nusse R.** Mechanisms of Wnt signaling in development. *Annu Rev Cell Dev Biol*. 1998; 14: 59–88.
40. **Clevers H.** Wnt/beta-catenin signaling in development and disease. *Cell*. 2006; 127: 469–80.
41. **He TC, Sparks AB, Rago C, *et al.*** Identification of c-MYC as a target of the APC pathway. *Science*. 1998; 281: 1509–12.
42. **Tetsu O, McCormick F.** Beta-catenin regulates expression of cyclin D1 in colon carcinoma cells. *Nature*. 1999; 398: 422–6.
43. **He TC, Chan TA, Vogelstein B, *et al.*** PPARdelta is an APC-regulated target of nonsteroidal anti-inflammatory drugs. *Cell*. 1999; 99: 335–45.
44. **Gong Y, Slee RB, Fukai N, *et al.*** LDL receptor-related protein 5 (LRP5) affects bone accrual and eye development. *Cell*. 2001; 107: 513–23.

45. **Little RD, Recker RR, Johnson ML.** High bone density due to a mutation in LDL-receptor-related protein 5. *N Engl J Med*. 2002; 347: 943–4; author reply 4.
46. **Boyden LM, Mao J, Belsky J, *et al.*** High bone density due to a mutation in LDL-receptor-related protein 5. *N Engl J Med*. 2002; 346: 1513–21.
47. **Chen Y, Whetstone HC, Lin AC, *et al.*** Beta-catenin signaling plays a disparate role in different phases of fracture repair: implications for therapy to improve bone healing. *PLoS Med*. 2007; 4: e249.
48. **Kahler RA, Westendorf JJ.** Lymphoid enhancer factor-1 and beta-catenin inhibit Runx2-dependent transcriptional activation of the osteocalcin promoter. *J Biol Chem*. 2003; 278: 11937–44.
49. **de Boer J, Siddappa R, Gaspar C, *et al.*** Wnt signaling inhibits osteogenic differentiation of human mesenchymal stem cells. *Bone*. 2004; 34: 818–26.
50. **Boland GM, Perkins G, Hall DJ, *et al.*** Wnt 3a promotes proliferation and suppresses osteogenic differentiation of adult human mesenchymal stem cells. *J Cell Biochem*. 2004; 93: 1210–30.
51. **van der Horst G, van der Werf SM, Farih-Sips H, *et al.*** Downregulation of Wnt signaling by increased expression of Dickkopf-1 and -2 is a prerequisite for late-stage osteoblast differentiation of KS483 cells. *J Bone Miner Res*. 2005; 20: 1867–77.
52. **Kahler RA, Galindo M, Lian J, *et al.*** Lymphocyte enhancer-binding factor 1 (Lef1) inhibits terminal differentiation of osteoblasts. *J Cell Biochem*. 2006; 97: 969–83.
53. **Tu X, Joeng KS, Nakayama KI, *et al.*** Noncanonical Wnt signaling through G protein-linked PKCdelta activation promotes bone formation. *Dev Cell*. 2007; 12: 113–27.
54. **Chang J, Sonoyama W, Wang Z, *et al.*** Noncanonical Wnt-4 signaling enhances bone regeneration of mesenchymal stem cells in craniofacial defects through activation of p38 MAPK. *J Biol Chem*. 2007; 282: 30938–48.
55. **Lengner CJ, Lepper C, van Wijnen AJ, *et al.*** Primary mouse embryonic fibroblasts: a model of mesenchymal cartilage formation. *J Cell Physiol*. 2004; 200: 327–33.
56. **Luo Q, Kang Q, Song WX, *et al.*** Selection and validation of optimal siRNA target sites for RNAi-mediated gene silencing. *Gene*. 2007; 395: 160–9.
57. **He TC, Zhou S, da Costa LT, *et al.*** A simplified system for generating recombinant adenoviruses. *Proc Natl Acad Sci USA*. 1998; 95: 2509–14.
58. **Luo J, Deng ZL, Luo X, *et al.*** A protocol for rapid generation of recombinant adenoviruses using the AdEasy system. *Nat Protoc*. 2007; 2: 1236–47.
59. **Zhou L, An N, Jiang W, *et al.*** Fluorescence-based functional assay for Wnt/beta-catenin signaling activity. *Biotechniques*. 2002; 33: 1126–8.
60. **He TC.** Distinct osteogenic activity of BMPs and their orthopaedic applications. *Journal of Musculoskeletal & Neuronal Interactions*. 2005; 5: 363–6.
61. **Morin PJ, Sparks AB, Korinek V, *et al.*** Activation of beta-catenin-Tcf signaling in colon cancer by mutations in beta-catenin or APC. *Science*. 1997; 275: 1787–90.
62. **Luu HH, Zhang R, Haydon RC, *et al.*** Wnt/beta-catenin signaling pathway as a novel cancer drug target. *Curr Cancer Drug Targets*. 2004; 4: 653–71.
63. **Yoshizawa T, Takizawa F, Iizawa F, *et al.*** Homeobox protein MSX2 acts as a molecular defense mechanism for preventing ossification in ligament fibroblasts. *Mol Cell Biol*. 2004; 24: 3460–72.
64. **Gordon MD, Nusse R.** Wnt signaling: multiple pathways, multiple receptors, and multiple transcription factors. *J Biol Chem*. 2006; 281: 22429–33.
65. **Sparks AB, Morin PJ, Vogelstein B, *et al.*** Mutational analysis of the APC/beta-catenin/Tcf pathway in colorectal cancer. *Cancer Res*. 1998; 58: 1130–4.
66. **Ducy P, Zhang R, Geoffroy V, *et al.*** Osf2/Cbfa1: a transcriptional activator of osteoblast differentiation. *Cell*. 1997; 89: 747–54.
67. **Ducy P, Karsenty G.** Two distinct osteoblast-specific cis-acting elements control expression of a mouse osteocalcin gene. *Mol Cell Biol*. 1995; 15: 1858–69.
68. **Nohe A, Keating E, Knaus P, *et al.*** Signal transduction of bone morphogenetic protein receptors. *Cell Signal*. 2004; 16: 291–9.
69. **Nakashima A, Katagiri T, Tamura M.** Cross-talk between Wnt and bone morphogenetic protein 2 (BMP-2) signaling in differentiation pathway of C2C12 myoblasts. *J Biol Chem*. 2005; 280: 37660–8.
70. **Katoh M.** Networking of WNT, FGF, Notch, BMP, and Hedgehog signaling pathways during carcinogenesis. *Stem Cell Rev*. 2007; 3: 30–8.
71. **Xiao G, Jiang D, Ge C, *et al.*** Cooperative interactions between activating transcription factor 4 and Runx2/Cbfa1 stimulate osteoblast-specific osteocalcin gene expression. *J Biol Chem*. 2005; 280: 30689–96.
72. **Reinhold MI, Naski MC.** Direct interactions of Runx2 and canonical Wnt signaling induce FGF18. *J Biol Chem*. 2007; 282: 3653–63.
73. **Rawadi G, Vayssiere B, Dunn F, *et al.*** BMP-2 controls alkaline phosphatase expression and osteoblast mineralization by a Wnt autocrine loop. *J Bone Miner Res*. 2003; 18: 1842–53.
74. **Chen Y, Whetstone HC, Youn A, *et al.*** Beta-catenin signaling pathway is crucial for bone morphogenetic protein 2 to induce new bone formation. *J Biol Chem*. 2007; 282: 526–33.
75. **Mbalaviele G, Sheikh S, Stains JP, *et al.*** Beta-catenin and BMP-2 synergize to promote osteoblast differentiation and new bone formation. *J Cell Biochem*. 2005; 94: 403–18.
76. **Nishita M, Hashimoto MK, Ogata S, *et al.*** Interaction between Wnt and TGF-beta signalling pathways during formation of Spemann's organizer. *Nature*. 2000; 403: 781–5.
77. **Hu MC, Piscione TD, Rosenblum ND.** Elevated SMAD1/beta-catenin molecular complexes and renal medullary cystic dysplasia in ALK3 transgenic mice. *Development*. 2003; 130: 2753–66.
78. **Hussein SM, Duff EK, Sirard C.** Smad4 and beta-catenin co-activators functionally interact with lymphoid-enhancing factor to regulate graded expression of Msx2. *J Biol Chem*. 2003; 278: 48805–14.
79. **Hu MC, Rosenblum ND.** Smad1, beta-catenin and Tcf4 associate in a molecular complex with the Myc promoter in dysplastic renal tissue and cooperate to control Myc transcription. *Development*. 2005; 132: 215–25.
80. **Gaur T, Lengner CJ, Hovhannisyan H, *et al.*** Canonical WNT signaling promotes osteogenesis by directly stimulating Runx2 gene expression. *J Biol Chem*. 2005; 280: 33132–40.
81. **MacDonald BT, Joiner DM, Oyserman SM, *et al.*** Bone mass is inversely proportional to Dkk1 levels in mice. *Bone*. 2007; 41: 331–9.
82. **Li X, Liu P, Liu W, *et al.*** Dkk2 has a role in terminal osteoblast differentiation and mineralized matrix formation. *Nat Genet*. 2005; 37: 945–52.
83. **Holmen SL, Zylstra CR, Mukherjee A, *et al.*** Essential role of beta-catenin in postnatal bone acquisition. *J Biol Chem*. 2005; 280: 21162–8.

84. **Day TF, Guo X, Garrett-Beal L, *et al.*** Wnt/beta-catenin signaling in mesenchymal progenitors controls osteoblast and chondrocyte differentiation during vertebrate skeletogenesis. *Dev Cell*. 2005; 8: 739–50.
85. **Glass DA, 2nd, Bialek P, Ahn JD, *et al.*** Canonical Wnt signaling in differen-tiated osteoblasts controls osteoclast differentiation. *Dev Cell*. 2005; 8: 751–64.
86. **Hill TP, Spater D, Taketo MM, *et al.*** Canonical Wnt/beta-catenin signaling prevents osteoblasts from differentiating into chondrocytes. *Dev Cell*. 2005; 8: 727–38.
87. **Tamai K, Semenov M, Kato Y, *et al.*** LDL-receptor-related proteins in Wnt signal transduction. *Nature*. 2000; 407: 530–5.
88. **Bodine PV, Billiard J, Moran RA, *et al.*** The Wnt antagonist secreted frizzled-related protein-1 controls osteoblast and osteocyte apoptosis. *J Cell Biochem*. 2005; 96: 1212–30.
89. **Kato M, Patel MS, Levasseur R, *et al.*** Cbfa1-independent decrease in osteoblast proliferation, osteopenia, and persistent embryonic eye vascularization in mice deficient in Lrp5, a Wnt coreceptor. *J Cell Biol*. 2002; 157: 303–14.
90. **Morvan F, Boulukos K, Clement-Lacroix P, *et al.*** Deletion of a single allele of the Dkk1 gene leads to an increase in bone formation and bone mass. *J Bone Miner Res*. 2006; 21: 934–45.
91. **Li J, Sarosi I, Cattley RC, *et al.*** Dkk1-mediated inhibition of Wnt signaling in bone results in osteopenia. *Bone*. 2006; 39: 754–66.